2006

Thermal stability and crystallization kinetics of mechanically alloyed TiC/Ti-based metallic glass matrix composite

Laichang Zhang
University of Wollongong, laichang@uow.edu.au

J. Xu
Chinese Academy of Science

J Eckert
Technische Universitat Darmstadt

Thermal stability and crystallization kinetics of mechanically alloyed Ti C Ti -based metallic glass matrix composite

Lai-Chang Zhang, Jian Xu, and Jürgen Eckert

Citation: Journal of Applied Physics **100**, 033514 (2006); doi: 10.1063/1.2234535
View online: http://dx.doi.org/10.1063/1.2234535
View Table of Contents: http://scitation.aip.org/content/aip/journal/jap/100/3?ver=pdfcov
Published by the AIP Publishing

Thermal stability and crystallization kinetics of mechanically alloyed TiC/Ti-based metallic glass matrix composite

Lai-Chang Zhang[a)]
FG Physikalische Metallkunde, FB 11 Material- und Geowissenschaften, Technische Universität Darmstadt, Petersenstraße 23, D-64287 Darmstadt, Germany

Jian Xu
Shenyang National Laboratory for Materials Science, Institute of Metal Research, Chinese Academy of Science, 72 Wenhua Road, Shenyang 110016, China

Jürgen Eckert
FG Physikalische Metallkunde, FB 11 Material- und Geowissenschaften, Technische Universität Darmstadt, Petersenstraße 23, D-64287 Darmstadt, Germany

(Received 13 March 2006; accepted 17 May 2006; published online 7 August 2006)

A Ti-based metallic glass matrix composite with 10 vol % TiC is synthesized by mechanical alloying. The thermal stability and crystallization kinetics of the metallic glass and composite powders are investigated by differential scanning calorimetry in the mode of isochronal heating and isothermal annealing. The isothermal transformation kinetics is analyzed by the Kolmogorov-Johnson-Mehl-Avrami equation. The values of the Avrami exponent calculated for low crystallization volume fractions imply that the crystallization of both types of powders is governed by diffusion-controlled three-dimensional growth. The mean activation energy of crystallization for the composite is slightly lower than that of the Ti-based metallic glass. The addition of 10 vol % TiC particles into a Ti-based metallic glass matrix may slightly affect the crystallization kinetics of the glassy matrix. © *2006 American Institute of Physics*. [DOI: 10.1063/1.2234535]

I. INTRODUCTION

Metallic glass matrix composites have been developed to improve the ductility or strength of monolithic metallic glasses that fail catastrophically in a brittle manner.[1] Powder processing technologies (i.e., mechanical alloying and gas atomization) are attractive alternative routes to synthesize glassy matrix composites compared with direct cooling from the melt.[2–5] This is especially important for the alloy systems with insufficient glass-forming ability to obtain bulk samples upon slow cooling, such as Al- and Ti-based alloys.[6,7] Metallic glasses can be deformed by viscous flow resulting from the significant decrease of their viscosity in the supercooled liquid region,[8,9] which is defined as the temperature interval (ΔT_x) between the glass transition temperature (T_g) and the onset temperature of crystallization (T_x). Metallic glass matrix composites in many multicomponent alloy systems with a sizable supercooled liquid region have been achieved through gas atomization[4,5] or mechanical alloying.[10–13] Examples are ductile metal/metallic glass matrix composites[4,5] and ceramic/metallic glass matrix composites.[10–13] Using the viscous flow in the supercooled liquid region, some metallic glass matrix composites have been consolidated, which show excellent mechanical properties combining high strength and ductility.[4,5]

Crystallization studies have been carried out on ball milled metallic glass matrix composites.[13–15] However, most of the investigations have focused on Zr-based metallic glass matrix composites, and little work has been reported on the crystallization kinetics of Ti-based metallic glass composites with second particles. Moreover, the metallic glass and/or corresponding composite powders may crystallize during powder consolidation if the consolidation conditions are not well controlled.[16] On the other hand, the detailed analysis of the thermal stability and crystallization kinetics of the metallic glasses and/or composite powders is the key to explore the optimal parameters for the consolidation of the powders into bulk form. It should be noted that even with partial or complete nanocrystallization during consolidation, the product might still be interesting in terms of its properties. This makes the investigation of kinetics even more relevant. For example, Ti-based nanostructured crystalline materials (solid solution) are of strong interest for their excellent combined mechanical properties.[17,18] Therefore, it is expected that the Ti-based composites will have excellent mechanical properties if the amorphous phase partially or completely nanocrystallizes into the structure with ductile solid solution (i.e., α-Ti or β-Ti) + partial amorphous phase rather than the mixture of brittle intermetallics. Accordingly, it is a crucial issue whether the alloys have an adequate thermal stability of the supercooled liquid against crystallization or not to provide a wide "temperature-time" window for subsequent powder consolidation. In addition, a study of crystallization from the original full glassy powder is important not only to achieving the glassy consolidates but also to arriving at desirable nanocrystalline alloy by using the crystallization process. Therefore, a detailed understanding of the crystallization kinetics is a prerequisite not only for optimizing the consolidation

[a)]Author to whom correspondence should be addressed; electronic mails: lczhangimr@gmail.com and l.zhang@phm.tu-darmstadt.de

parameters but also for the applications, because the thermal stability against crystallization determines the potential use as structural materials.

In the present work, we report on the formation of a $Ti_{50}Cu_{18}Ni_{22}Al_4Sn_6$ metallic glass composite reinforced with 10 vol % TiC particles by mechanical alloying. Our focus is to investigate the effect of the TiC particles on the thermal stability and crystallization kinetics of the metallic glass and composite powders.

II. EXPERIMENT

Starting from elemental pieces with a purity higher than 99.9 wt %, the master alloy with a nominal composition of $Ti_{50}Cu_{18}Ni_{22}Al_4Sn_6$ was prepared by arc melting under a Ti-gettered argon atmosphere. The alloyed button was then crushed into fragments, with sizes less than ~500 μm and in flake shape, and used as starting material for ball milling. The fragments were identified to be a mixture of several intermetallic phases including NiTi, Ti_2Cu, and Ti_3Sn.[19] About 10 vol % of TiC particles (Alfa Aesar) with a purity higher than 99.9 wt % and particle sizes smaller than 45 μm were blended with the prealloyed fragments. The blended powder mixtures were loaded together with hardened steel balls in a hardened steel vial in an argon-filled glovebox with less than 1 ppm O_2 and H_2O. A ball-to-powder weight ratio of 5:1 was employed. The ball milling was performed with a SPEX 8000 shaker mill cooled by forced flowing air. For all the samples discussed in this paper, the milling time was fixed at 32 h. This time was chosen according to the previous work on this alloy system[20] to assure that the milling has proceeded sufficiently long for the samples to reach a steady state, but short enough to avoid excessive contamination from the milling media.

The phase formation of the as-milled powders was characterized by x-ray diffraction (XRD) using a Rigaku D/max 2400 diffractometer with monochromated Cu $K\alpha$ radiation ($\lambda = 0.1542$ nm). The glass transition and crystallization behaviors were analyzed using a Perkin-Elmer Diamond differential scanning calorimeter (DSC) under flowing purified argon, with a heating rate of 40 K/min. A second heating run under identical conditions was used to determine the base line. To determine the onset temperature of the glass transition (T_g), the samples were heated to the temperature of T_g +20 K to reach a relaxed state for resolving the heat flow change in the DSC scan. The T_g of the samples was defined as the intersection of the tangents to the DSC trace above and below the initial change in the base line slope.[21] Isothermal DSC measurements were carried out by heating to different temperatures in the supercooled liquid region with a heating rate of 40 K/min, then holding for 60 min.

The iron and oxygen contents in the ball milled products were analyzed to be no more than 0.50 and 0.15 wt %, respectively, using inductively coupled plasma emission spectroscopy (ICP10P, ARL) and a LECO TC-436 system, respectively. Thus, the chemical atomic composition of the amorphous phase is approximately $Ti_{49.49}Cu_{17.81}Ni_{21.77}Al_{3.96}Sn_{5.94}Fe_{0.50}O_{0.53}$, which is very close to the nominal composition of $Ti_{50}Cu_{18}Ni_{22}Al_4Sn_6$.

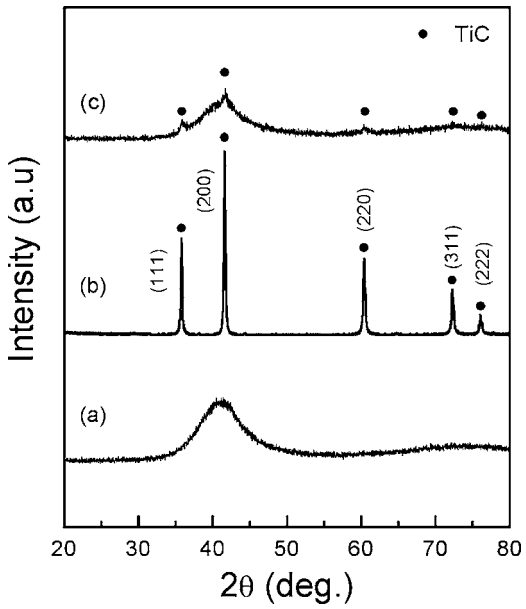

FIG. 1. XRD patterns of (a) $Ti_{50}Cu_{18}Ni_{22}Al_4Sn_6$ metallic glass, (b) the initial TiC particles, and (c) the composite with 10 vol % TiC.

III. RESULTS AND DISCUSSION

Figure 1 shows the XRD patterns of the ball milled $Ti_{50}Cu_{18}Ni_{22}Al_4Sn_6$ alloy and the composite with 10 vol % TiC particles. For comparison, the XRD pattern of the initial TiC powder is also given [Fig. 1(b)]. For the ball milled Ti-based alloy without any addition [Fig. 1(a)], only broad diffuse scattering maxima of a metallic glass phase are observed, and no diffraction peaks of any crystalline phases are detected. It indicated that a single metallic glass phase formed in the ball milled $Ti_{50}Cu_{18}Ni_{22}Al_4Sn_6$ powder, which is proved by the transmission electron microscopy observation in Ref. 19. For the composite powders [Fig. 1(c)], only TiC diffraction peaks are superimposed on the broad diffuse scattering maxima of the Ti-based metallic glass phase. No considerable amounts of other crystalline phases are visible within the sensitivity limit of x-ray diffraction. There are no changes in the position of the TiC reflections and the metallic glass scattering maximum, which suggest that there is no obvious chemical reaction between the matrix alloy and the added TiC particles.

Figure 2 displays the DSC scans in the mode of isochronal heating with a heating rate of 40 K/min for the Ti-based metallic glass and the composite. Both the metallic glass and the composite powders crystallize through a single step. The crystallized products are identified to be a cubic NiTi-type phase and an unidentified phase.[19] A distinct glass transition prior to crystallization and a wide supercooled liquid region can be observed for both samples. For comparison purposes, the thermal properties obtained from the isochronal DSC measurements for both samples are summarized in Table I, including the glass transition temperature T_g, the onset temperature of crystallization T_x, the peak temperature of the crystallization reaction T_p, the width of the supercooled liquid region ΔT_x, and the heat release of crystallization ΔH_x. As seen from Table I, there are no visible changes in the T_g(=705 K), T_x(=771 K), T_p(=776 K), and ΔT_x(=66 K) val-

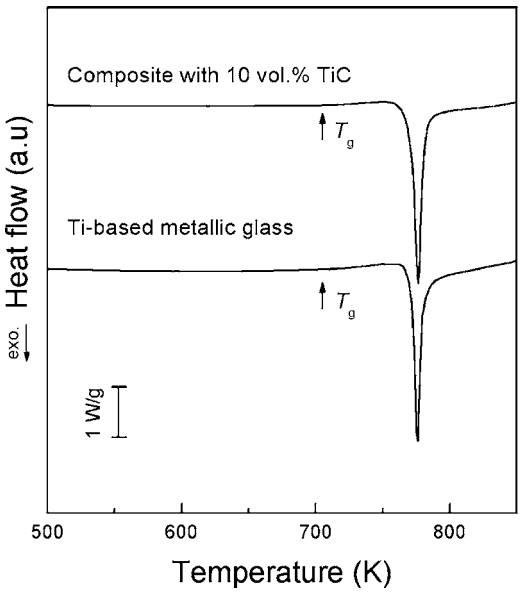

FIG. 2. Isochronal DSC scans of the ball milled $Ti_{50}Cu_{18}Ni_{22}Al_4Sn_6$ metallic glass and the composite with 10 vol % TiC (heating rate of 40 K/min).

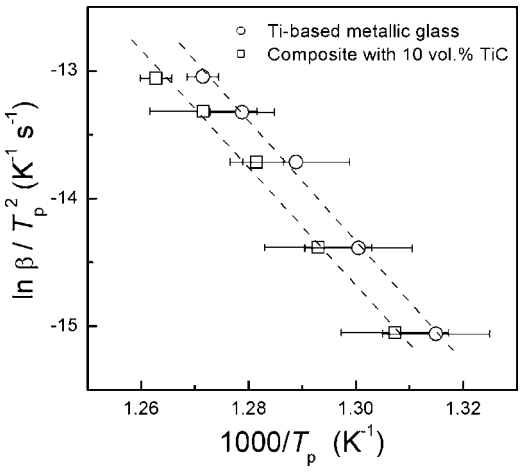

FIG. 3. Kissinger plots obtained from DSC scans with different heating rates for the Ti-based metallic glass and composite powders with 10 vol % TiC.

ues between the metallic glass and the composite. It has been reported that the thermal stability of the metallic glass matrix alloy can be affected in the course of the formation of the composites with respect to the metallic glasses without second-phase particulates, due to the chemical interaction between the dispersoids and the metallic glass matrix.[10–13] The supercooled liquid region is either enlarged or reduced, depending on the chemical interaction between the matrix and the ceramic agent, and on the volume fraction of addition. For example, 5 vol % oxide particles[11] or 10 vol % nitride particles[13] added in a Zr-based metallic glass matrix increase the thermal stability of the metallic glass matrix. In contrast, in the boride/Ti-based metallic glass matrix composites,[10] 10 vol % of the borides do not affect the thermal stability of the Ti-based metallic glass matrix, but larger volume fractions of boride additions improve the thermal stability of the metallic glass matrix. Accordingly, the identical values of T_g, T_p, and T_x for the present composite containing 10 vol % TiC with respect to the $Ti_{50}Cu_{18}Ni_{22}Al_4Sn_6$ metallic glass again imply that the chemical composition of the metallic glass phase in the TiC-containing composite is the same as that in the initial glassy alloy, or that there is no obvious chemical reaction between the added TiC particles and the metallic glass matrix in the TiC-containing composite.

To further estimate the thermal stability of the Ti-based metallic glass alloys with and without TiC particles, the activation energies (E_x) of crystallization for both samples can be evaluated by means of the Kissinger equation:[22]

$$\ln\left(\frac{\beta}{T_p^2}\right) = -\frac{E_x}{RT} + C. \tag{1}$$

Here, β is the heating rate, R the gas constant, T_p the crystallization peak temperature, and C is a constant. The different crystallization peak temperatures can be obtained from DSC curves recorded in continuous heating mode using different heating rates. The Kissinger plots, $\ln(\beta/T_p^2)$ vs $1/T_p$, of the Ti-based metallic glass and the composite are shown in Fig. 3. From the slope of the straight line the activation energy for crystallization is obtained. The activation energies calculated for the Ti-based metallic glass and composite powders are 392±17 and 382±22 kJ/mol, respectively (Table II). The obtained activation energies are in good agreement with those of other Ti-based metallic glass alloys, i.e., $Ti_{45}Zr_5Cu_5Ni_{45}$ glassy ribbons (380 kJ/mol) (Ref. 23) and bulk $Ti_{53}Cu_{27}Ni_{12}Zr_3Al_7Si_3B_1$ metallic glass (378 kJ/mol).[24] The nearly identical activation energies indicate that the composition of the metallic glass matrix in the composite is almost identical to that of the Ti-based metallic glass powder without TiC addition. This suggests that there is almost no chemical reaction between the TiC particles and the metallic glass matrix in the composite, which can also be proved from the XRD patterns (Fig. 1) and the DSC curves (Fig. 2) of the glassy and composite powders. This is of vital importance for the synthesis of bulk Ti-based materials by subsequent consolidation.

Figures 4(a) and 4(b) show the isothermal DSC traces recorded at several different temperatures for the ball milled

TABLE I. Glass transition temperature (T_g), onset (T_x) and peak (T_p) temperatures of crystallization, extension of the supercooled liquid region (ΔT_x), and heat release of crystallization (ΔH_x) obtained from isochronal DSC measurements (heating rate of 40 K/min).

Sample	T_g (K)	T_x (K)	T_p (K)	ΔT_x (K)	ΔH_x (kJ/mol)
$Ti_{50}Cu_{18}Ni_{22}Al_4Sn_6$	705±1	771±1	776±1	66±1	2.68±0.14
With 10 vol % TiC	705±1	771±1	776±1	66±1	2.43±0.19

TABLE II. Avrami exponent (n) and activation energy of crystallization ($E_{x\tau}$) in terms of incubation time during isothermal annealing and the activation energy of crystallization (E_x) determined from a Kissinger plot for the ball milled Ti-based metallic glass and the composite with 10 vol % TiC.

Sample	Temperature range (K)	n	$x_c(t,T)$ range	$E_{x\tau}$ (kJ/mol)	E_x (kJ/mol)
$Ti_{50}Cu_{18}Ni_{22}Al_4Sn_6$	735–755	2.5–3.3	0.05–0.60	399±55	392±17
With 10 vol % TiC	723–750	2.1–2.8	0.05–0.60[a]	384±10	382±22

[a]0.05–0.40 was used for the composite at 723 K.

Ti-based metallic glass phase and the composite with 10 vol % TiC particles, respectively. The annealing temperatures are chosen in the supercooled liquid region of the corresponding samples. All DSC curves exhibit a single exothermic peak after passing a certain incubation period (τ), which is related to the crystallization event in the mode of constant-rate heating. The incubation time as well as the time required for complete crystallization become shorter when annealing at higher temperatures. This can be ascribed to the higher atomic mobility at higher temperatures, which causes concentration fluctuations necessary for large-scale crystallization to set in. To explore suitable parameters for subsequent powder consolidation of the Ti-based metallic glass powders and the composite into bulk form in the supercooled liquid region, the temperature-time-transformation (TTT) diagram for the onset of crystallization of both samples has been constructed for both powders by plotting the variation of the incubation time at various temperatures in the supercooled liquid region during isothermal annealing, as shown in Fig. 5. For both the Ti-based metallic glass and the composite, the supercooled liquid state can be maintained at T_g +20 K for more than 400 s until crystallization occurs. Such a "temperature-time window" is quite similar to what was formed for the ball milled TiB_2/Ti-based amorphous matrix composites[10] and the gas-atomized powders of ZrAlNiCu,[16] CuTiZrNiSi,[25] and ZrNbCuNiAl (Vitreloy 106a) (Ref. 26) metallic glasses. For these alloys, bulk metallic glasses have been fabricated through powder consolidation in the temperature-time window.[16,25,26] The wide temperature-time window for both of the powders implies that subsequent powder consolidation in the supercooled liquid region should be feasible.

It is assumed that the volume fraction of the crystalline phase formed during the crystallization process associated with the DSC peak, or the volume fraction of the remaining metallic glass phase, can be estimated from the corresponding enthalpy release assuming that the area under the DSC peak is proportional to the volume fraction of crystals or residual amorphous phase, respectively.[27,28] Therefore, in the isothermal DSC scans, the transformed volume fraction, $x_c(t,T)$, up to any time t is proportional to the fractional areas of the exothermic peak. Hence, the crystallized volume fraction during the isothermal annealing process can be accurately determined by measuring the area of the exothermic peak. The crystallized fractions $x_c(t,T)$ after time t at a certain temperature T for the glassy and composite powders are derived from the isothermal DSC curves in Figs. 4(a) and 4(b) by assuming that $x_c(t,T)$ is proportional to the integrated enthalpy,

$$x_c(t,T) = \int_0^t h(t,T)dt \Big/ \int_0^\infty h(t,T)dt. \tag{2}$$

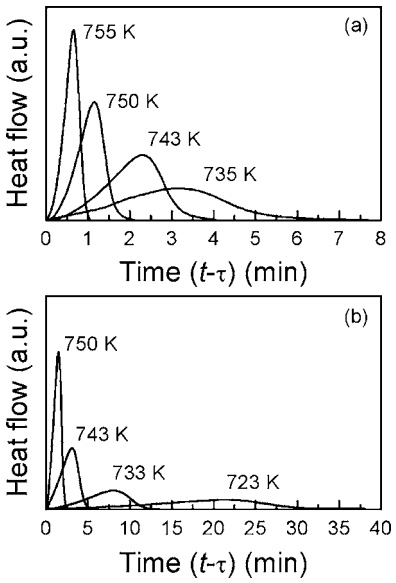

FIG. 4. Isothermal DSC scans at different temperatures for the ball milled (a) $Ti_{50}Cu_{18}Ni_{22}Al_4Sn_6$ metallic glass and (b) the composite with 10 vol % TiC.

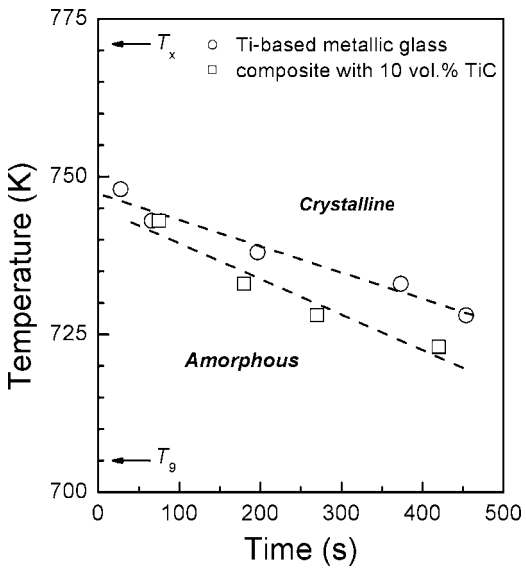

FIG. 5. TTT diagram for the onset of crystallization for $Ti_{50}Cu_{18}Ni_{22}Al_4Sn_6$ metallic glass and the composite with 10 vol % TiC, heated to selected temperatures at a heating rate of 40 K/min.

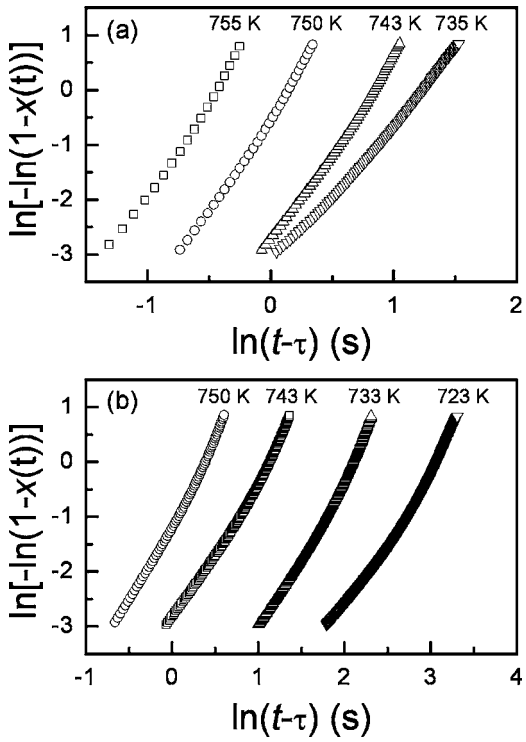

FIG. 6. KJMA plots of the ball milled (a) $Ti_{50}Cu_{18}Ni_{22}Al_4Sn_6$ metallic glass powders and (b) the composite with 10 vol % TiC.

The isothermal crystallization kinetics of the metallic glass phase can be usually analyzed in terms of the generalized theory of the well-known Kolmogorov-Johnson-Mehl-Avrami (KJMA) equation[29,30] for a phase transition:

$$x_c(t,T) = 1 - \exp[-k(t-\tau)^n] \tag{3}$$

or

$$\ln\{-\ln[1 - x_c(t,T)]\} = n \ln k + n \ln(t-\tau), \tag{4}$$

where $x_c(t,T)$ is the volume fraction of crystallized phases after annealing time t, τ is the incubation period of transient nucleation, k is a temperature-dependent kinetic parameter, and n is the Avrami exponent, which is a significant parameter to describe the crystallization mechanism, such as nucleation and growth behavior, and varies from 1 to 4.[31] For diffusion-controlled growth, one may have the following cases: $1<n<1.5$ indicates growth of particles with an appreciable initial volume, $n=1.5$ indicates growth of particles with a nucleation rate close to zero, $1.5<n<2.5$ reflects growth of particles with decreasing nucleation rate, $n=2.5$ reflects growth of particles with constant nucleation rate, and $n>2.5$ pertains to the growth of small particles with an increasing nucleation rate.[32] A KJMA plot of $\ln\{-\ln[1-x_c(t,T)]\}$ vs $\ln(t-\tau)$ yields a straight line with slop n and intercept $n \ln k$.

The KJMA plots of the mechanically alloyed Ti-based metallic glass and the composite with 10 vol % TiC particles in the range of $0.05 \leqslant x_c(t,T) \leqslant 0.90$ are shown in Figs. 6(a) and 6(b), respectively. The Avrami exponent n and the reaction rate constant k can be calculated from the slopes and the intercepts of the lines. However, a continuously curved line rather than a simple linearity is demonstrated for both powders, similar as it is widely observed in the other alloys.[13,33,34] Calka and Radlinski[35] have demonstrated that evaluating the mean Avrami exponent over a range of the volume fractions transformed may be inappropriate and may be even misleading. Nonlinear Avrami plots can result from the inhomogeneous distribution of nuclei during crystallization.[36] The Avrami exponent n at high $x_c(t,T)$ and the average Avrami exponent will not reflect the nucleation rate and/or the growth morphology correctly, if the nuclei are distributed inhomogeneously, while the local Avrami exponents at low $x_c(t,T)$ are actually unaffected by the inhomogeneity of the distribution of nuclei, when the inhomogeneity of the distribution of nuclei is not high enough. Accordingly, one can still use the local Avrami exponents at low $x_c(t,T)$ to determine the nucleation rate and/or growth morphology.[36,37] Therefore, the Avrami exponent n values for both types of samples were calculated in the low crystallization volume fraction range of $0.05 \leqslant x_c(t,T) \leqslant 0.60$ [except for the composite powder at 723 K for which $0.05 \leqslant x_c(t,T) \leqslant 0.40$ was used]. The data in this range are almost on a straight line with a correlation coefficient better than 0.999. The values of the Avrami exponent n range from 2.5 to 3.3 for the Ti-based metallic glass and they vary from 2.1 to 2.8 for the 10 vol % TiC-containing composite (Table II). The Avrami exponent n, which relates to the operating crystallization mechanism,[31] gives detailed information on the nucleation and growth behavior. Crystallization occurs by long-range diffusion of atoms in the supercooled liquid and this is a diffusion-controlled process. Therefore, the n values of 2.5–3.3 for the Ti-based metallic glass and 2.1–2.8 for the composite powder suggest that their crystallization is governed by a nucleation rate that increases with time. The Avrami exponent values also indicate that the rearrangement of atoms in the supercooled liquid becomes easier with increasing annealing temperature. The growth of nuclei results in compositional fluctuations in the neighborhood. The composition changes result in enhanced nucleation rates at regions adjacent to the growing nuclei, which cause a chain-reaction-like process leading to an increasing nucleation rate.[15]

As shown before, it is inappropriate to describe the crystallization mechanism by using the mean Avrami exponent derived from the nonlinear KJMA plot in the whole range of volume fraction. An alternative method of examining the isothermal DSC results is to evaluate the local value of the Avrami exponent, N_{loc}, which is defined as[35]

$$N_{\mathrm{loc}} = \partial \ln\{-\ln[1 - x_c(t,T)]\}/\partial \ln(t-\tau), \tag{5}$$

as a function of crystallized volume fraction $x_c(t,T)$. Such an analysis can highlight the changes in reaction kinetics during the progress of crystallization. In order to investigate the details of the crystallization process of the Ti-based metallic glass and the composite, the local Avrami exponents of both powders were calculated using Eq. (5). Figure 7 shows the local value of the Avrami exponent as a function of the crystallization volume fraction for the ball milled metallic glass and composite powders that were isothermally annealed at 750 K in the range of $0.005 \leqslant x_c(t,T) \leqslant 0.995$. It can be seen that the value of N_{loc} varies significantly with crystallization volume fraction over the whole crystallization process. For

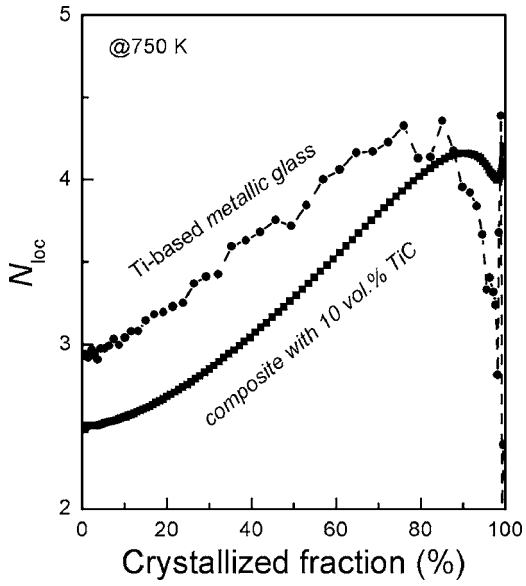

FIG. 7. Variation of the local Avrami exponent with crystallization volume fraction for the $Ti_{50}Cu_{18}Ni_{22}Al_4Sn_6$ metallic glass powders and the composite with 10 vol % TiC annealed at 750 K.

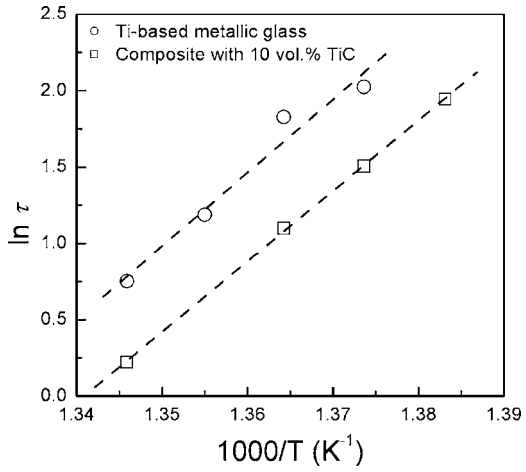

FIG. 8. Arrhenius plots of $\ln \tau$ vs $1/T$ for the ball milled Ti-based metallic glass and the composite powder with 10 vol % TiC.

the Ti-based metallic glass, the local Avrami exponent in the early stage of crystallization is around 2.90, indicating diffusion-controlled three-dimensional growth and zero nucleation rate;[35] the bulk crystallization stage dominates over the whole range of transformation. The value of N_{loc} gradually increases with $x_c(t,T)$ during the crystallization process up to 4.0 and then begins to decrease to around 3.0 at $x_c(t,T) \approx 0.80$. The changes of the local Avrami exponent of the Ti-based metallic glass suggest that the nucleation is nonsteady. The observed increase in the value of the Avrami exponent in the last stage of crystallization may be due to errors derived from the isothermal DSC results.[38] For the TiC-containing composite powder, the local Avrami exponent in the early stage of crystallization is about 2.5, implying a constant nucleation rate at the initial crystallization stage.[35] With increasing extent of transformation, the contribution of bulk crystallization to the overall transformation steadily increases leading to higher N_{loc} values, implying that nucleation and growth in the bulk of the samples dominates during crystallization. The value of N_{loc} increases to a value about 4, which means that the nucleation rate increases with annealing time, and so does the increasing rate of nucleation rate. N_{loc} decreases after reaching a maximum value, which shows a decrease of the increasing rate of nucleation. In the later stages of crystallization, the value of the Avrami exponent decreases, suggesting a reduced nucleation rate. This can be attributed to nucleation saturation and three-dimensional growth of crystalline nuclei, leading to subsequent crystal impingement.[35,39,40]

The activation energy for the crystallization process can also be determined in terms of the incubation period τ at different temperatures during isothermal annealing using the Arrhenius equation for a thermally activated process:[41,42]

$$\tau = \tau_0(-E_{x\tau}/RT), \tag{6}$$

where τ_0 is a constant and $E_{x\tau}$ is the activation energy for crystallization. Figure 8 shows the plot of $\ln \tau$ vs $1/T$ for both samples, which yields a straight line. From the slope, the activation energies $E_{x\tau}$ for crystallization are calculated as 399 ± 55 and 384 ± 10 kJ/mol (Table II) for the Ti-based metallic glass and the composite, respectively. As seen from Table II, there are no essential differences in the activation energies between those evaluated using the Arrhenius equation in isothermal annealing and those obtained by isochronal annealing as revealed by Kissinger analysis (Fig. 3) for the Ti-based metallic glass with and without TiC particles. However, compared with the mean activation energies of Ti-based alloy without and with TiC addition estimated from the above-mentioned methods, it is easy to find that the mean activation energies of the composite with 10 vol % TiC are slightly lower than those of the Ti-based metallic glass even though the energy difference is quite small (about 10–15 kJ/mol). This indicates that the interfaces between the glassy matrix and the TiC particles may act as potential heterogeneous nucleation sites, which generally decreases the activation barrier for crystallization,[43] even though there are no distinct changes in the XRD patterns (Fig. 1) and DSC scans (Fig. 2) between the Ti-based metallic glass and the composite with TiC. It should be noted that a very close Avrami exponent $n = 2.6 \pm 0.1$ was also reported in the Al/Ni multiplayer films prepared by solid-state interdiffusion reaction.[44] It is assumed that the nucleated Al_3Ni grows and coalesces into a continuous layer and then thickens by diffusion-limited process with kinetic characteristics and the presence of a significant amount of interfacial impurities has a strong influence on the nucleation and growth of the intermetallic Al_3Ni phase. This scenario is very similar to the current work that there are also a mount of interfaces between the TiC particle and the glassy matrix phase in the composite, resulting in that the preexisting TiC particles might serve as potential nucleation sites of crystals during crystallization. This may be occur if there is a fast interface-limited two-dimensional growth (mediated by interfacial diffusion) of the crystalline phase preferentially nucleated around the TiC particle (quickly wetting the particle), then followed/accompanied by diffusion-limited growth in the three-dimensional growth. Under this condition, the Avrami exponent n is also about 2.5. Although this probability

should be proven by further detailed investigations, it can be a sign for this scenario that the activation energy of the composite with 10 vol % TiC slightly reduces compared with that of Ti-based metallic glass without TiC addition.

IV. SUMMARY

Ti-based metallic glass matrix composite containing 10 vol % TiC particles can be formed by ball milling. The addition of TiC particles does not affect the calorimetric glass transition temperature, as well as the peak and onset temperatures of the crystallization of the metallic glass matrix. Both the Ti-based metallic glass and the TiC-containing composite powders have a wide "temperature-time window" for subsequent consolidation of the powders into bulk materials in the supercooled liquid state. The values of the Avrami exponent calculated in the lower crystallization volume fraction region imply that the crystallization of both types of powders is governed by diffusion-controlled three-dimensional growth. The activation energy of crystallization determined from the Kissinger analysis and the Arrhenius equation for both powders show that the composite has slightly lower activation energy. The addition of 10 vol % TiC particles into the Ti-based metallic glass may slightly affect the crystallization kinetics of the glassy phase and the TiC particles may act as potential heterogeneous nucleation sites.

ACKNOWLEDGMENTS

The authors thank S. Venkataraman and Dr. H. B. Lu for useful discussions. Financial support by the EU via the RTN-network on "ductile bulk metallic glass composites" (MRTN-CT-2003-504692) is gratefully acknowledged. One of the author (L.C.Z.) is very grateful for the financial support of the Alexander von Humboldt Foundation.

[1]M. Telford, Mater. Today **7**, 36 (2004).
[2]M. Seidel, J. Eckert, and L. Schultz, J. Appl. Phys. **77**, 5446 (1995).
[3]M. Seidel, J. Eckert, I. Bächer, M. Reibold, and L. Schultz, Acta Mater. **48**, 3657 (2000).
[4]D. H. Bae, M. H. Lee, D. H. Kim, and D. J. Sordelet, Appl. Phys. Lett. **83**, 2312 (2003).
[5]M. H. Lee, D. H. Bae, D. H. Kim, and D. J. Sordelet, J. Mater. Res. **18**, 2101 (2003).
[6]A. Inoue, Prog. Mater. Sci. **43**, 365 (1998).
[7]A. Inoue, Mater. Sci. Forum **312–314**, 307 (1999).
[8]E. Bakke, R. Busch, and W. L. Johnson, Appl. Phys. Lett. **67**, 3260 (1995).
[9]N. Nishiyama and A. Inoue, Mater. Trans., JIM **40**, 64 (1999).
[10]L. C. Zhang, Z. Q. Shen, and J. Xu, J. Non-Cryst. Solids **351**, 2277 (2005).
[11]J. Eckert, M. Seidel, A. Kübler, U. Klement, and L. Schultz, Scr. Mater. **38**, 595 (1998).
[12]B. Bartusch, F. Schurack, and J. Eckert, Mater. Trans., JIM **43**, 1979 (2002).
[13]C. R. Zhou and J. Xu, J. Non-Cryst. Solids **297**, 131 (2002).
[14]S. Deledda, J. Eckert, and L. Schultz, Scr. Mater. **46**, 31 (2002).
[15]S. Venkataraman, E. Rozhkova, J. Eckert, L. Schultz, and D. J. Sordelet, Intermetallics **13**, 833 (2005).
[16]Y. Kawamura, H. Kato, A. Inoue, and T. Masumoto, Appl. Phys. Lett. **67**, 2008 (1995).
[17]Y. T. Zhu, J. Y. Huang, J. Gubicza, T. Ungár, Y. M. Wang, E. Ma, and R. Z. Valiev, J. Mater. Res. **18**, 1908 (2003).
[18]B. B. Sun, M. L. Sui, Y. M. Wang, G. He, J. Eckert, and E. Ma, Acta Mater. **54**, 1349 (2006).
[19]L. C. Zhang, Z. Q. Shen, and J. Xu, Mater. Sci. Eng., A **394**, 204 (2005).
[20]L. C. Zhang and J. Xu, Mater. Lett. **56**, 615 (2002).
[21]L. C. Zhang, J. Xu, and E. Ma, J. Mater. Res. **17**, 1743 (2002).
[22]H. E. Kissinger, Anal. Chem. **29**, 1702 (1957).
[23]X. Q. Guo, D. V. Louzguine, and A. Inoue, Mater. Trans., JIM **42**, 2406 (2001).
[24]D. V. Louzguine and A. Inoue, J. Mater. Res. **14**, 4426 (1999).
[25]J. Robertson, J. T. Im, I. Karaman, K. T. Hartwig, and I. E. Anderson, J. Non-Cryst. Solids **317**, 144 (2003).
[26]I. Karaman, J. Robertson, J. T. Im, S. N. Mathaudhu, Z. P. Luo, and K. T. Hartwig, Metall. Mater. Trans. A **35**, 247 (2004).
[27]A. Inoue, H. Tomioka, and T. Masumoto, J. Mater. Sci. **18**, 153 (1983).
[28]L. C. Zhang, Z. Q. Shen, and J. Xu, J. Mater. Res. **18**, 2141 (2003).
[29]C. V. Thompson, A. L. Greer, and F. Spaepen, Acta Metall. **31**, 1883 (1983).
[30]K. F. Kelton, J. Non-Cryst. Solids **163**, 283 (1993).
[31]R. D. Doherty, in *Physical Metallurgy*, edited by R. W. Cahn and P. Haasen (North Holland, Amsterdam, 1996), p. 1363.
[32]L. Liu, Z. E. Wu, W. H. Wang, Y. Zhang, M. X. Pan, and D. Q. Zhao, Appl. Phys. Lett. **75**, 2392 (1999).
[33]A. L. Greer, Acta Metall. **30**, 171 (1982).
[34]M. M. Nicolaus, H. R. Sinning, and F. Haessner, Mater. Sci. Eng., A **150**, 101 (1992).
[35]A. Calka and A. P. Radlinski, Mater. Sci. Eng. **97**, 241 (1988).
[36]N. X. Sun, X. D. Liu, and K. Lu, Scr. Mater. **34**, 1201 (1996).
[37]S. Deledda, J. Eckert, and L. Schultz, Mater. Res. Soc. Symp. Proc. **754**, CC6.19 (2003).
[38]Z. Z. Yuan, X. D. Chen, B. X. Wang, and Z. J. Chen, J. Alloys Compd. **399**, 166 (2005).
[39]K. Lu and J. T. Wang, J. Non-Cryst. Solids **117–118**, 716 (1990).
[40]G. J. Fan, M. X. Quan, Z. Q. Hu, W. Löser, and J. Eckert, J. Mater. Res. **14**, 3765 (1999).
[41]F. E. Luborsky, Mater. Sci. Eng. **28**, 139 (1977).
[42]D. Kawase, A. P. Tsai, A. Inoue, and T. Masumoto, Appl. Phys. Lett. **62**, 137 (1993).
[43]H. C. Yim, R. Busch, and W. L. Johnson, J. Appl. Phys. **83**, 7993 (1998).
[44]E. Ma, C. V. Thompson, and L. A. Clevenger, J. Appl. Phys. **69**, 2211 (1991).